

Constrained Path-Planning Control of Unmanned Surface Vessels via Ant-Colony Optimization

Ming-Yuan Gao^{1,2}, Bin-Bin Hu¹, Bin Liu¹, Ning Qiu³, Hai-Tao Zhang^{*,1}

1. School of Artificial Intelligence and Automation, and State Key Lab of Digital Manufacturing Equipment and Technology, Huazhong University of Science and Technology, Wuhan 430074, P.R. China
E-mail: zht@mail.hust.edu.cn
2. China-EU Institute for Clean and Renewable Energy, Huazhong University of Science and Technology, Wuhan 430074, P.R. China
3. Chinese Acad Sci, Chinese Acad Sci Key Lab Ocean & Marginal Sea Geo, South China Sea Inst Oceanol, Guangzhou 510301, Guangdong, Peoples R China

Abstract: This paper proposes a constrained path-planning scheme for the unmanned surface vessel (USV) via ant-colony optimization. First, a multi-grid map is modeled and established along the kinematics of the USV body suffered by limited energy. A typical ant-colony optimization algorithm is afterwards designed to achieve the energy-saving path planning for narrow channels of water areas. Finally, real lake experiments with HUSTER-12s USV are conducted to verify the effectiveness of the proposed path-planning algorithm.

Key Words: Constrained path planning, ant-colony optimization, unmanned surface vessel (USV)

1 Introduction

Recently, due to the high efficient development and utilization of marine resources, increasing attention has been devoted to the ocean industry. As an unmanned intelligent platform on the sea, unmanned surface vehicle (USV) is applicable in patrol, reconnaissance, water quality monitoring surrounding and many other aspects [1–5], which has been a hot research topic in various countries. However, due to the sophisticated environment and complex tasks, more recent efforts have been devoted to the research of the intelligent USV path planning.

Notably, the first step of path planning is map modeling, which is to abstract the located USV map. Therein, the map modeling could be separated into grid method, visibility graph method, voronoi diagram method, free space method, topological diagram method, etc [6]. Then, with the assistance of the abstract map, it suffices to plan path, including classic A* algorithm, D* algorithm, etc [6]. Furthermore, due to the challenging issues in the path-planning task, more intelligent bionics algorithms have been developed, such as colony algorithm [7], particle swarm optimization algorithm [8] and genetic algorithm [9], etc.

The challenge of USV path-planning problem lies mainly in the constrained environment, underactuated and nonlinear kinematics of the USV. In this pursuit, Cao *et al.* [10] developed a path-planning method based on voronoi diagram and improved genetic algorithm, using the principle of hierarchical path planning. Zhang *et al.* [11] proposed a USV optimal path planning method based on genetic algorithm and simulated annealing algorithm. Liu *et al.* [12] designed a USV path planning method based on ant colony algorithm (ACA) and clustering algorithm (CA). Afterwards, Wang *et al.* [13]

proposed an improved USV path planning based on the ant colony algorithm that combines the wolf group allocation principle and the maximum and minimum ant system. Wang *et al.* [6] studied a USV global path planning problem with grid method and ant colony algorithm.

However, in actual exploration and reconnaissance, the energy carried by USV is always limited, which may cause immeasurable losses in the harsh water environment. It thus becomes an urgent task to consider energy consumption in the path-planning task of the USV. As the pioneer works, Zhang [14] firstly proposed a global path planning via the typical A* algorithm, in which the impact of ocean currents on energy consumption is considered. Then, Song *et al.* [15] developed a multi-layered fast marching method to be applied to USV path planning, which considered the impact of the time-varying marine environment on USV energy consumption. Dhanushka *et al.* [16] proposed a graph search-based method for USV and AUV to plan time and energy optimization paths in static and time-varying flow fields. Nevertheless, most of the previous works only focused on simulation and have not considered the real experiments. It now becomes highly necessary to propose a practical constrained path-planning method for USV.

To this end, this paper presents a USV path planning method under multiple constraints. Compared with the existing results, the main contributions of this paper are: 1) A grid map modeling method based on a multi-grid USV model is proposed, taking into account the rigid body model, dynamic model and energy limitation. 2) Based on the above grid map, an ant colony algorithm with multiple constraints is proposed for USV energy-saving path planning in narrow waterways of lakes. 3) Experiments were carried out on the Songshan Lake experimental platform to verify the effectiveness of the algorithm.

The structure of this paper is as follows: Section 2 introduces the model and problem description; Section 3 presents the path planning algorithm; real lake experiment are conducted in Section 4; the conclusion is drawn in Section 5.

This work was supported by the National Natural Science Foundation of China (NNSFC) under Grants U1713203, 51729501, 62003145, and in part by Natural Science Foundation of Hubei Province under Grant 2019CFA005, and in part by the Program for Core Technology Tackling Key Problems of Dongguan City under Grant 2019622101007, and in part by the Fundamental Research Funds for Central Universities, HUST: 2020JY-CXJJ070. Corresponding author: Hai-Tao Zhang.

2 Modeling and Problem Description

2.1 USV Modeling

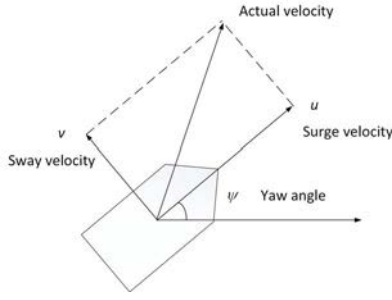


Fig. 1: The illustration of the USV's dynamic

Consider the USV shown in Fig. 1, ignoring the USV's motion in heave, roll and pitch, the kinematics model [1, 4] between the earth coordinate system and the USV coordinate system is as follows:

$$\begin{cases} \dot{x} = u \cos(\psi) - v \sin(\psi) \\ \dot{y} = u \sin(\psi) + v \cos(\psi) \\ \dot{\psi} = r \end{cases} \quad (1)$$

where (x, y) represents the position of the centroid of the USV, and ψ represents the heading angle of the USV in the earth coordinate system. (u, v, r) respectively represent the surge velocity, sway velocity and yaw velocity of USV. For the USV in the medium speed mode (1-3m/s), after a lot of experiments and parameter identification, we can get the simplified three-degree-of-freedom dynamic model [1-3] of the USV as follows:

$$\begin{cases} \dot{\psi} = r \\ \dot{u} = k_1 u + k_2 v r + k_3 \tau_1 \\ \dot{r} = k_4 r + k_5 \tau_2 \\ \dot{v} = k_6 v + k_7 u r \end{cases} \quad (2)$$

where k_i denotes the parameters related to inertia and hydro-dynamic damping. τ_1 and τ_2 represent propeller speed and the steering angle respectively, which are the main control parameters.

2.2 Grid Map Modeling

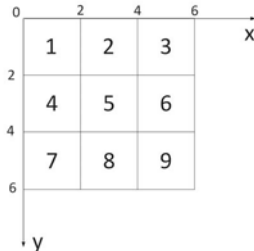


Fig. 2: The rectangular coordinate method and the serial number method

The grid method is a widely used intelligent algorithm in USV path planning. The basic idea of the algorithm is: Regarding the obstacles in the space as known conditions, the

path planning space is transformed into grid units with binary information. As shown in Fig. 2, the grid is identified by a combination of rectangular coordinate method and serial number method. The advantage of the coordinate method is that it can intuitively determine the location of each path point, and the path length can be directly calculated in a rectangular coordinate system. The advantage of the serial number method is that in the iteration of the algorithm, a position can be simply and uniquely represented by a number, which can significantly simplify the calculation.

Consider that the passable information of all grids is stored in a two-dimensional map information matrix. Generally, the obstacle grid is represented by 1, and the free grid is represented by 0. We assume that the scale of the grid is M rows and N columns, and the side length of the grid is a , then the map information matrix G is:

$$G_{i,j} = \begin{cases} 1, & \text{obstacle grid} \\ 0, & \text{free grid} \end{cases} \quad (3)$$

where $i = 0, 1, \dots, M-1, j = 0, 1, \dots, N-1$.

For the grid numbered p , its position (x_p, y_p) in the rectangular coordinate system can be denoted as:

$$\begin{cases} x_p = a \times [\text{mod}(p, n) - a/2] \\ y_p = a \times [m + a/2 - \text{ceil}(p/m)] \end{cases} \quad (4)$$

The subscripts (i, j) in the matrix $G_{i,j}$ can be obtained by the following formula:

$$\begin{cases} j = \text{mod}(p, N) \\ i = \text{floor}(p/N) \end{cases} \quad (5)$$

where mod is the remainder function, ceil is the round-up function, and floor is the round-down function.

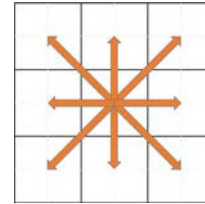


Fig. 3: The octree search strategy

Fig. 3 shows the octree search strategy as a grid transfer method, which means the USV moves freely to adjacent grids in 8 directions. Suppose there is a USV that moves from grid p with coordinates (i, j) to grid q with coordinates (m, n) then the following constraints are given:

$$\begin{cases} G_{m,n} = 0 \\ d_{pq} = \sqrt{(x_p - x_q)^2 + (y_p - y_q)^2} = a \text{ or } \sqrt{2}a \end{cases} \quad (6)$$

where d_{pq} is the movement length of USV.

2.3 Energy Consumption Modeling

In a grid map, we assume that the energy consumption of USV is measured in three aspects [14, 15]:

1) The energy consumption of the USV with uniform linear motion in still water is related to path length.

$$E_{\text{straight}} = \sum_{i=1}^N L_i F / \eta, \quad (7)$$

where L_i is the path length of the USV in the i -th trajectory, F is the thrust of the propeller, and η is the conversion efficiency of the propeller.

- 2) The turning energy consumption of the USV is related to the steering angle:

$$E_{\text{turn}} = \sum_{i=1}^{N-1} k\theta_i, \quad (8)$$

where θ_i is the steering angle of the i -th turn of the USV in the grid map, and k is the correlation coefficient.

- 3) The impact of wind, waves and currents on USV is related to the work of environmental forces.

$$E_{\text{env}} = \sum_{i=1}^N L_i \tau_i, \quad (9)$$

where τ_i is the environmental force on the i th trajectory of the USV.

In summary, the overall energy consumption of the USV in the grid map is represented by the following equation:

$$\begin{aligned} E &= E_{\text{straight}} + E_{\text{turn}} + E_{\text{env}} \\ &= k_1 L + k_2 \theta + k_3 L \tau, \end{aligned} \quad (10)$$

where k_1 , k_2 , k_3 are the coefficients related to the actual energy consumption of the USV, L is the total path length of the USV movement, θ is the sum of all steering angles in a path of the USV, and τ is the environmental force.

2.4 Problem Description

Consider the situation where a USV is performing a mission in a small lake. A USV with a length of L and a width of W needs to bypass obstacles to reach the target location. On the way, it needs to pass through a narrow waterway of width H , satisfying $L > H > W$.

As shown in Fig. 4(a), the single-grid USV model cannot cross obstacles because the USV is a long and narrow rigid body. According to the dynamics model of USV, the USV has strong nonlinearity and underdrive which means it cannot make sharp turns and reverses. In addition, most lake USVs are small and electrically driven, with very limited energy. This is a path planning problem with optimal energy consumption:

$$\min E$$

subject to

$$\begin{aligned} a &\leq H \\ G_{\vec{v}_x t_i, \vec{v}_y t_i} &= 0 \\ (\vec{v}_x t)^2 + (\vec{v}_y t)^2 &= (x_e - x_s)^2 + (y_e - y_s)^2 \end{aligned} \quad (11)$$

along the trajectory (2) where E is the energy consumption of USV, a is the side length of the grid, G is the map information matrix, \vec{v}_x and \vec{v}_y are the velocity vectors of USV on the x -axis and y -axis respectively, t_i is the moving time of USV, $i \in \mathbb{N}$, t is the time when the USV reaches the end, x_s and y_s represent the x and y coordinates of the starting point, and x_e , y_e represent the x and y coordinates of the end point respectively. These constraints will be considered in the passable information of grids in the following part.

3 Path Planning Algorithm

Aiming at the constraints of the rigid body model, dynamic model and energy finiteness of the USV in the above scenario, this paper proposes a multi-grid model of USV combined with ant colony algorithm for path planning.

3.1 Multi-grid Model of USV

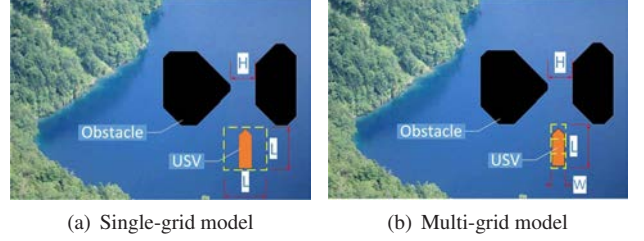


Fig. 4: The USV crosses the narrow waterway in the lake

Consider a USV with an aspect ratio of 3:1. The rigid body model is represented by three grids instead of one grid. As shown in Fig. 4(b), due to the improved grid accuracy, the unmanned boat can easily pass through the narrow Waterway.

Still consider the grid map which has M rows and N columns. The USV moves from grid p to grid q . The coordinates of grid p are (i, j) , and the coordinates of grid q are (m, n) . This multi-grid model of USV has eight attitudes as shown in the Fig. 5.

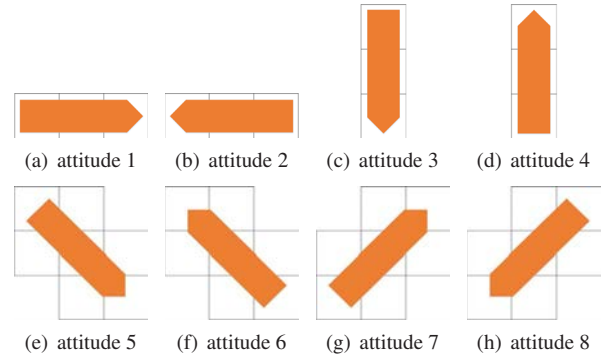


Fig. 5: Eight attitudes of USV

We define the grid passable information of each attitude of the USV as follows:

$$\left\{ \begin{aligned} G_{p, \text{attitude1}} &= G_{p, \text{attitude2}} \\ &= G_{i,j} + G_{i,j-1} + G_{i,j+1} = 0 \\ G_{p, \text{attitude3}} &= G_{p, \text{attitude4}} \\ &= G_{i,j} + G_{i-1,j} + G_{i+1,j} = 0 \\ G_{p, \text{attitude5}} &= G_{p, \text{attitude6}} \\ &= G_{i,j} + G_{i,j-1} + G_{i,j+1} \\ &\quad + G_{i-1,j} + G_{i+1,j} + G_{i-1,j-1} \\ &\quad + G_{i+1,j+1} = 0 \\ G_{p, \text{attitude7}} &= G_{p, \text{attitude8}} \\ &= G_{i,j} + G_{i,j-1} + G_{i,j+1} \\ &\quad + G_{i-1,j} + G_{i+1,j} + G_{i-1,j+1} \\ &\quad + G_{i+1,j-1} = 0 \end{aligned} \right. \quad (12)$$

For the grid transfer rules of the USV, We stipulate:

- The USV must move at most one grid each time.
- USV can turn up to 90 each time.

For each initial attitude, the movement of the USV in the grid can be roughly divided into three situations, which are described below with three examples.

- 1) The USV doesn't turn: As shown in Fig. 6(a), the USV maintains attitude 3 and moves forward, grids satisfy:

$$G_{p,attitude1} + G_{q,attitude1} = 0. \quad (13)$$

- 2) The USV turns 45 degrees: As shown in Fig. 6(b), the USV rotates from attitude 4 to attitude 8, grids satisfy:

$$G_{p,attitude1} + G_{p,attitude5} + G_{q,attitude5} = 0. \quad (14)$$

- 3) The USV turns 90 degrees: As shown in Fig. 6(c), the USV rotates from attitude 4 to attitude 2, grids satisfy:

$$G_{p,attitude1} + G_{p,attitude5} + G_{p,attitude3} + G_{q,attitude3} = 0. \quad (15)$$

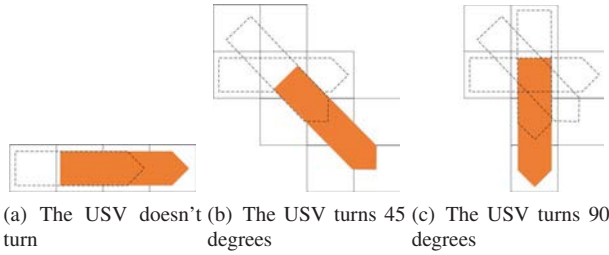


Fig. 6: Three cases of USV transfer in the grid

Therefore, we can calculate the passable information of the grid every time the USV moves. In fact, in the iteration of the algorithm, we will not judge the transfer rule of the grid every time, which will greatly waste computer performance. The method we take is to solve a cost matrix in advance, which is a three-dimensional matrix and stores the cost of each grid reaching each of its adjacent barrier-free grids at each attitude angle. The cost matrix is calculated by the following equation:

$$Cost_{p,q,attitude} = E_{p,q,attitude}, \quad (16)$$

where $E_{p,q,attitude}$ is the energy consumption of this movement, which can simply be calculated using the equation(10).

3.2 Ant Colony Algorithm

Ant Colony Algorithm [7] is an intelligent algorithm proposed by Dorigo M inspired by ants foraging. During the foraging process, ants will leave a hormone called pheromone on the path, which is related to a predefined cost. When the cost is smaller, the path will have more pheromone, and the probability of ants choosing this path will be higher. At the same time, when the number of ants on a path increases, the pheromone on this path will increase, which is a positive feedback. Ant colony algorithm has excellent positive feedback, self-organization, parallelism, robustness and other advantages. The algorithm in this paper improves the grid model, the heuristic function, and

the pheromone update method of the algorithm, so that the search path is in line with the actual engineering application.

For the grid transfer rules, on the one hand, the grids that have been passed will be added to the tabu list and no longer selected. On the other hand, only grid transfers that meet the grid transfer rules can be allowed. Use p, q to represent the current and next grid, and $attitude$ to represent the current state of the USV. The grid transfer rules satisfy:

$$\begin{cases} Tab_{p,q} \neq 0 \\ Cost_{p,q,attitude} \neq 0 \end{cases} \quad (17)$$

The probability of grid transfer is the probability that an ant selects another optional grid as the next grid, which is calculated by the following equation:

$$P_{pq}^k = \begin{cases} \frac{\tau_{pq}^\alpha(t)\eta_{pq}^\beta(t)}{\sum_{s \in allowed_k} \tau_{ps}^\alpha(t)\eta_{ps}^\beta(t)}, & q \in allowed_k \\ 0, & q \notin allowed_k \end{cases} \quad (18)$$

In the formula, k is the ant number, t is the current time, $\tau_{pq}(t)$ is the pheromone function, and $\eta_{pq}(t)$ is the heuristic function. α and β are the weights of pheromone information and heuristic information respectively, and $allowed_k$ is the set of optional grids.

The heuristic function $\eta_{ij}(t)$ determines the final direction of the ant and expresses the attraction of the end point to ants. It is calculated by the following equation:

$$\eta_{pq}(t) = \frac{1}{d_{pq}}, \quad (19)$$

where d_{pq} is the length of the USV moving from grid p to grid q .

Every time all ants complete an iteration, the pheromone will be updated once. This update includes the enhancement of the new pheromone and the volatilization of the old pheromone. The pheromone update rules are as follows:

$$\begin{cases} \tau_{pq}(t+1) = (1-\rho) * \tau_{pq}(t) + \Delta\tau_{pq} \\ \Delta\tau_{pq} = \sum_{k=1}^n \Delta\tau_{pq}^k \end{cases}, 0 < \rho < 1 \quad (20)$$

where τ_{pq} represents the pheromone concentration on the path from grid p to grid q , and $\Delta\tau_{pq}^k$ represents the pheromone just released by ant k on the path from grid p to grid q . ρ is the pheromone volatilization factor, which determines how much pheromone volatilizes in this iteration.

Combined with the energy consumption model of USV, the following function is used for the pheromone update method:

$$\Delta\tau_{pq}^k(N) = \begin{cases} \frac{Q}{k_1 L + k_2 \theta + k_3 L \tau}, & (p, q) \text{ is the optimal path} \\ 0, & \text{others} \end{cases} \quad (21)$$

This heuristic function considers the energy consumption of USV from three aspects: path length, path smoothness, and environmental impact.

This paper uses the global pheromone update rule, which means that after each iteration, each segment of the optimal path is updated. The selection of the optimal path is based on the following fitness function

$$Fit_k = k_1 L + k_2 \theta + k_3 L \tau. \quad (22)$$

The path with the smallest value of the fitness function will be selected as the optimal path.

3.3 Algorithm Description

Consider the grid map matrix is G , the adjacency cost matrix is $Cost$, the tabu list is Tab , the set of optional grids is Opt . The total number of iterations is K , the total number of ants is M , the current grid number is p , the next grid number is q , the start grid number is $Start$, the end grid number is End . The probability of reaching each grid is p_{pq}^k , the ant pheromone is τ . The pseudo-code description of the algorithm is shown in Algorithm 1.

Algorithm 1 Path Planning Algorithm

```

1: Initialize G and parameters
2: Create Cost and Tab
3: for p,q,attitude do
4:    $Cost_{p,q,attitude} = k_1L + k_2\theta + k_3L\tau$ 
5: end for
6: for k = 1 : K do
7:   for m = 1 : M do
8:     while  $q \neq End$  and  $Opt \neq 0$  do
9:       if  $Cost_{p,q,attitude} \neq 0$  and  $Tab_{p,q} \neq 0$  then
10:        add q to Opt
11:      end if
12:      Caculate  $p_{pq}^k$ 
13:      Use roulette to select q
14:       $Totalcost = Totalcost + Cost_{p,q,attitude}$ 
15:       $Tab_{p,q} = 0$ 
16:    end while
17:    if  $q = end$  and  $TotalCost < MinCost$  then
18:      Update optimal path
19:    end if
20:  end for
21:  Update  $\tau$ 
22: end for

```

4 Experiment

4.1 Experimental Platform Introduction

The experiment used the USV platform located in Songshan Lake, Dongguan, Guangdong, China. The USV is connected to the base station on the dock via a wireless network and exchanges data such as position, direction angle and speed in real time. The USV used in this experiment is HUSTER-12s. As shown in Fig. 7(a), it is a 120cm USV equipped with an embedded controller, a motor driver, a differential GPS, a wireless transmission module, a water jet propulsion and a rudder. Refer to [1] for detailed model parameters.

In order to complete the USV path planning task, the construction of the host software is an important task. The host software is deployed in the PC, which connects the base station on the shore and the USV in the lake through a wireless network. Its main uses are:

- Real-time reception and display of USV status information.
- When the user selects the starting point and ending point on the electronic map, the software automatically plans the path based on the path planning algorithm and displays it on the screen.
- Send the control information to the USV to perform trajectory tracking.

The host software interface is shown in Fig. 7(b).

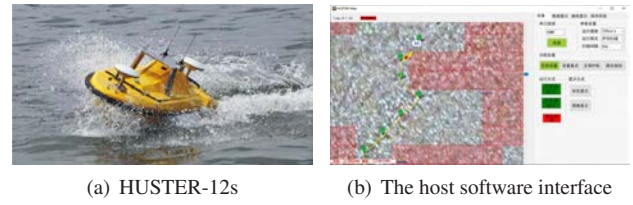
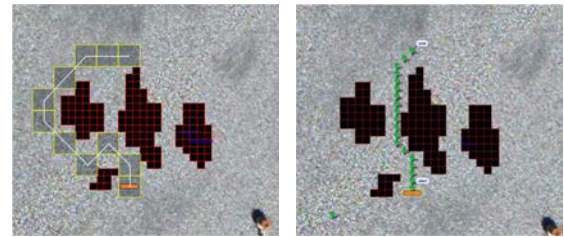


Fig. 7: The experimental platform

4.2 Experiment Introduction



Fig. 8: The location of virtual obstacles and the direction of virtual wind, waves and currents

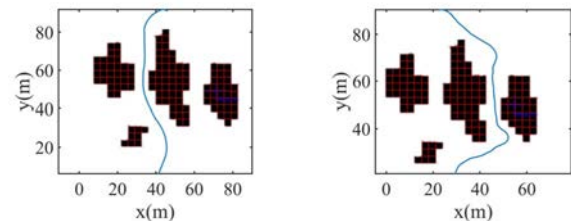


(a) Algorithm A (b) Algorithm B



(c) Algorithm C

Fig. 9: Path planning results



(a) Algorithm B (b) Algorithm C

Fig. 10: The actual trajectory of USV

The experiment was carried out in a water area of Songshan Lake. As shown in Fig. 8, several virtual obstacles were set in the host software. Consider the USV crossing these obstacles from south to north. In addition, the force of

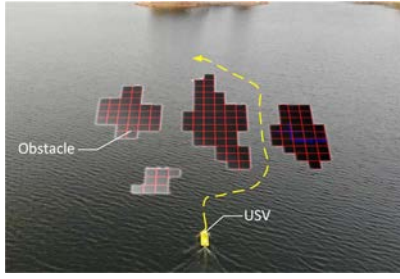


Fig. 11: The snapshot of the experiment

the virtual wind, wave, current and their direction is shown in Fig. 8. In real experiments, these virtual environmental effects are taken into account in the calculation of energy consumption.

The algorithm parameters are selected as follows: iteration number $K = 200$, number of ants $M = 80$, pheromone factor $\alpha = 1$, heuristic factor $\beta = 3$, initial pheromone $Q = 1$, pheromone volatilization factor $\rho = 0.3$, The parameters $k_1 = 1.0$, $k_2 = 0.51$, $k_3 = 1.5$, environmental force $F = 1N$, and the grid side length is 4m. Consider three algorithms separately:

- Algorithm A: The ant colony algorithm based on the USV's single-grid model
- Algorithm B: The ant colony algorithm based on the USV's multi-grid model without considering energy consumption.
- Algorithm C: The ant colony algorithm based on the USV's multi-grid model considering energy consumption.

As shown in Fig. 9(a), Algorithm A can only make a detour to pass the obstacles. Fig. 9(b), 9(c) show that the planning path of algorithm B, C calculated by the host software. Fig. 10 shows the actual trajectory of algorithm B, C in the lake. Fig. 11 shows a snapshot of the experiment. Finally, the comparative indicators of the planned path are shown in Table 1, which are calculated by the algorithm parameters and the paths planned by the host software. Obviously, The algorithm C proposed in this paper has great advantages in crossing narrow obstacles and saving energy.

Table 1: The comparative indicators of the planned path

	Algorithm A	Algorithm B	Algorithm C
Crossing obstacles	No	Yes	Yes
Path length (m)	149.82	78.63	101.25
Steering angle ($^{\circ}$)	450	225	270
Environmental work (J)	54.43	43.11	3.51
Energy consumption (J)	247.46	151.30	116.13

5 Conclusion

This paper proposes a constrained path-planning method with ant-colony algorithm. With such a proposed scheme, the USV fulfills path-planing and path-following missions with underactuated USV dynamics, nonlinear kinetics and limited energy. Lake experiments were conducted by the self-developed HUSTER-12s USVs to verify the effectiveness of the algorithm. Significantly, as the proposed method is more accurate and energy-efficient, it has application

potential for the path planning task with narrow channels formed by obstacles within aquatic areas.

References

- [1] B. Liu, Z. Chen, H.-T. Zhang, X. Wang, T. Geng, H. Su, and Z. Jin. Collective dynamics and control for multiple unmanned surface vessels. *IEEE Transactions on Control Systems Technology*, 28(6):254–2547, 2020.
- [2] B.-B. Hu, H.-T. Zhang, and J. Wang. Multiple-target surrounding and collision avoidance of a second-order nonlinear multi-agent system. *IEEE Transactions on Industrial Electronics*, in press, doi: 10.1109/TIE.2020.3000092.
- [3] B. Liu, H.-T. Zhang, H. Meng, D. Fu, and H. Su. Scanning-chain formation control for multiple unmanned surface vessels to pass through water channels. *IEEE Transactions on Cybernetics*, in press, doi: 10.1109/TCYB.2020.2997833.
- [4] B.-B. Hu, B. Liu, and H.-T. Zhang. Cooperative hunting control for multi-underactuated surface vehicles. In *37th Chinese Control Conference (CCC)*, pages 6602–6607. IEEE, 2018.
- [5] B.-B. Hu, H.-T. Zhang, B. Liu, H.-F. Meng, and G.-R. Chen. Distributed surrounding control of multiple unmanned surface vessels with varying interconnection topologies. *IEEE Transactions on Control Systems Technology*, in press, doi: 10.1109/TCST.2021.3057640.
- [6] Y.-H. Wang and C. Chi. Research on optimal planning method of usv for complex obstacles. In *2016 IEEE International Conference on Mechatronics and Automation*, 2016.
- [7] M. Dorigo, G. D. Caro, and L. M. Gambardella. Ant algorithms for discrete optimization. *Artificial Life*, 5(2):137–172, 1999.
- [8] R. Eberhart and J. Kennedy. A new optimizer using particle swarm theory. In *Mhs95 Sixth International Symposium on Micro Machine & Human Science*, 2002.
- [9] J. Holland. Adaptation in natural and artificial systems : an introductory analysis with application to biology. *Ann Arbor*, 6(2):126137, 1975.
- [10] C. Lu. Improved genetic algorithm for fast path planning of usv. In *Ninth International Symposium on Multispectral Image Processing and Pattern Recognition (MIPPR2015)*, 2015.
- [11] W. Zhang, Y. Xu, and J. Xie. Path planning of usv based on improved hybrid genetic algorithm. In *2019 European Navigation Conference (ENC)*, 2019.
- [12] X. Liu, Y. Li, J. Zhang, J. Zheng, and C. Yang. Self-adaptive dynamic obstacle avoidance and path planning for usv under complex maritime environment. *IEEE Access*, 7:114945–114954, 2019.
- [13] H. Wang, F. Guo, H. Yao, S. He, and X. Xu. Collision avoidance planning method of usv based on improved ant colony optimization algorithm (march 2019). *IEEE Access*, pages 1–1, 2019.
- [14] H.-H. Zhang, L. Gong, T. Chen, L. Wang, and X. Zhang. Global path planning methods of uuv in coastal environment. In *IEEE International Conference on Mechatronics & Automation*, 2016.
- [15] R. Song, Y. Liu, and R. Bucknall. A multi-layered fast marching method for unmanned surface vehicle path planning in a time-variant maritime environment. *Ocean Engineering*, 129(JAN.1):301–317, 2017.
- [16] D. Kularatne, S. Bhattacharya, and M. A. Hsieh. Going with the flow: a graph based approach to optimal path planning in general flows. *Autonomous Robots*, 42(7):1369–1387, 2018.